

Simple and efficient methods for the accurate evaluation of patterning effects in ultrafast photonic switches

Jing Xu,^{1,*} Yunhong Ding,^{1,2} Christophe Peucheret,¹ Weiqi Xue,¹ Jorge Seoane,¹ Beáta Zsigri,¹ Palle Jeppesen,¹ and Jesper Mørk¹

¹ DTU Fotonik, Department of Photonics Engineering, Ørstedts Plads, Building 343, DK-2800 Kgs. Lyngby, Denmark

² Wuhan National Laboratory for Optoelectronics, Huazhong University of Science and Technology, 430074, China

*Corresponding author: jinxu@fotonik.dtu.dk

Abstract: Although patterning effects (PEs) are known to be a limiting factor of ultrafast photonic switches based on semiconductor optical amplifiers (SOAs), a simple approach for their evaluation in numerical simulations and experiments is missing. In this work, we experimentally investigate and verify a theoretical prediction of the pseudo random binary sequence (PRBS) length needed to capture the full impact of PEs. A wide range of SOAs and operation conditions are investigated. The very simple form of the PRBS length condition highlights the role of two parameters, i.e. the recovery time of the SOAs as well as the operation bit rate. Furthermore, a simple and effective method for probing the maximum PEs is demonstrated, which may relieve the computational effort or the experimental difficulties associated with the use of long PRBSs for the simulation or characterization of SOA-based switches. Good agreement with conventional PRBS characterization is obtained. The method is suitable for quick and systematic estimation and optimization of the switching performance.

© 2010 Optical Society of America

OCIS codes: (070.4340) Nonlinear optical signal processing; (250.5980) Semiconductor optical amplifiers; (250.6715) Switching.

References and links

1. Y. Liu, E. Tangdiongga, Z. Li, H. de Waardt, A. M. J. Koonen, G. D. Khoe, X. Shu, I. Bennion, and H. J. S. Dorren, "Error-free 320-Gb/s all-optical wavelength conversion using a single semiconductor optical amplifier," *J. Lightwave Technol.* **25**, 103–108 (2007).
2. E. Tangdiongga, Y. Liu, H. de Waardt, G. D. Khoe, A. M. J. Koonen, H. J. S. Dorren, X. Shu, and I. Bennion, "All-optical demultiplexing of 640 to 40 Gbits/s using filtered chirp of a semiconductor optical amplifier," *Opt. Lett.* **32**, 835–837 (2007).
3. J. Leuthold, D. M. Marom, S. Cabot, J. J. Jaques, R. Ryf, and C. R. Giles, "All-optical wavelength conversion using a pulse reformatting optical filter," *J. Lightwave Technol.* **22**, 186–192 (2004).
4. M. L. Nielsen and J. Mørk, "Increasing the modulation bandwidth of semiconductor-optical-amplifier-based switches by using optical filtering," *J. Opt. Soc. Am. B* **21**, 1606–1619 (2004).
5. S. Kumar, B. Zhang, and A. E. Willner, "Elimination of data pattern dependence in SOA-based differential-mode wavelength converters using optically-induced birefringence," in *Optical Fiber Communication Conference and Exposition and The National Fiber Optic Engineers Conference, Technical Digest (CD)* (Optical Society of America, 2006), paper OThB3.

6. R. Giller, X. Yang, R. J. Manning, R. P. Webb, and D. Cotter, "Pattern effect mitigation in the turbo-switch," in International Conference on Photonics in Switching (2006).
7. J. Wang, A. Marculescu, J. Li, P. Vorreau, S. Tzadok, S. Ben Ezra, S. Tsadka, W. Freude, and J. Leuthold, "Pattern effect removal technique for semiconductor-optical-amplifier-based wavelength conversion," IEEE Photon. Technol. Lett. **19**, 1955–1957 (2007).
8. R. P. Webb, J. M. Dailey, and R. J. Manning, "Pattern compensation in SOA-based gates," Opt. Express **18**, 13502–13509 (2010).
9. F. J. MacWilliams and N. J. A. Sloane, "Pseudo-random sequences and arrays," Proc. IEEE **64**, 1715–1729 (1976).
10. A. V. Uskov, T. W. Berg, and J. Mørk, "Theory of pulse-train amplification without patterning effects in quantum-dot semiconductor optical amplifiers," IEEE J. Quantum Electron. **40**, 306–320 (2004).
11. J. Xu, X. Zhang, and J. Mørk, "Investigation of patterning effects in ultrafast SOA-based optical switches," IEEE J. Quantum Electron. **46**, 87–94 (2010).
12. T. Kobayashi, H. Yao, K. Amano, Y. Fukushima, A. Morimoto, and T. Sueta, "Optical pulse compression using high-frequency electrooptic phase modulation" IEEE J. Quantum Electron. **24**, 382–387 (1988).

1. Introduction

High-speed photonic switching is a key enabling technology for all-optical signal processing, which avoids optical-electrical-optical (O-E-O) conversion and therefore potentially allows superior operation speed and/or reduction of energy consumption compared to electronic switching. Among various physical switching mechanisms, optical nonlinearities in semiconductor optical amplifiers (SOAs) have been extensively studied. In spite of the slow carrier dynamics of SOAs, typically occurring on the time-scale of tens to hundreds of picoseconds, impressive demonstrations at 320 Gbit/s and 640 Gbit/s have been reported for all-optical wavelength conversion [1] and demultiplexing [2]. Operation at such high speeds is made possible by the fact that the linear part of the patterning effects (PEs) caused by the slow carrier recovery process can be effectively suppressed by properly filtering the output spectrum [3, 4]. This benefit may be exploited in an extremely simple structure, i.e. a single SOA followed by an optical filter, as shown in Fig. 1(a). This configuration has numerous advantages, including high stability, possibility of integration and low switching power. On the other hand, it is well known that such switches still suffer from nonlinear PEs [4] that are partly responsible for the large observed power penalties [1, 2] and would require additional effort to eliminate [5, 6, 7, 8]. As shown in Fig. 1(b), the PE defined for a non-inverted output waveform is the ratio between the maximum peak power and the minimum peak power of the output switched pulses. As a consequence of the carrier and gain transients in the SOA, the extent of the PE is therefore dependent on the random properties of the input data sequences.

In a laboratory environment, pseudo-random binary sequences (PRBS) are conventionally used to emulate random data that may be switched in real situations. PRBSs are favored in the sense that they appear random to the channel but are predictable to the tester, so that bit-error-ratios (BERs) can be computed. In general, the period of a typical shift-register PRBS is expressed as $2^n - 1$, where the bit-pattern length n is sufficient to describe the random properties of the sequence [9]. In order to properly characterize SOA-based switches with respect to the PEs, it is necessary to launch PRBSs with sufficiently large n so that the full extent of the slow SOA dynamics can be probed. This is not only challenging in numerical simulations, but also difficult in high-speed experiments where high bit rate test signals are generated using passive optical time multiplexing of lower bit-rate tributaries. It is therefore essential to be able to assess whether a given bit-pattern length is sufficient to predict the maximum PE. It is also desirable to develop simple alternative methods that are able to assess the full PEs without resorting to the use of long PRBSs, whose use in numerical simulations is prohibitive, or which are challenging to generate at high bit rates.

In our previous work [11] we theoretically proposed a lower bound limit for the bit-pattern

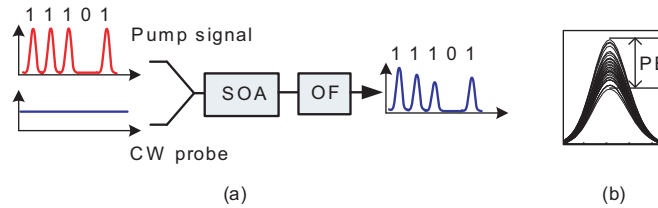


Fig. 1. (a) Ultrafast photonic switch based on SOA followed by offset filtering. The pump signal is used to switch the intensity of the probe, which may be exploited for wavelength conversion, optical time division demultiplexing, optical logic, etc. (b) Illustration and definition of patterning effects (PEs). SOA: semiconductor optical amplifier; OF: optical filter.

length that should be adopted in order to capture the maximum PE. In addition, an approach alternative to the use of PRBS patterns to estimate the maximum PE (referred to as the “periodic method”) was proposed and numerically validated. In this paper, the first experimental verification of the methods proposed in [11] is carried out over a wide selection of SOAs and different SOA operation conditions. Good agreement is obtained between the theoretical and experimental results, confirming the generality and power of the proposed methods.

2. Experimental validation

2.1. Experimental setup

Fig. 2 shows the setup used for PE measurements. The pulse source consists of a continuous wave (CW) laser centered at 1548.32 nm, a Mach-Zehnder modulator (MZM) used to carve 50% duty cycle pulses, and a phase modulator (PM) followed by a length of standard single mode fibre (SMF) for pulse compression [12]. The PM is driven by a 40 GHz radio frequency (RF) signal with $V_{pp} = 2V_{\pi}$, where V_{pp} is the peak-to-peak voltage of the RF signal and V_{π} is the half-wave voltage of the PM. After transmission through 250 m SMF, a train of pulses having a full-width at half-maximum (FWHM) of 2.6 ps and a repetition rate of 40 GHz is obtained. By using a shorter fiber length, i.e. 150 m, pulses with a FWHM of 7.2 ps can be achieved. The pulse train is further data modulated by another MZM driven by a bit-pattern generator (BPG). By programming the BPG, either PRBS patterns at different bit rates or pulse trains with different repetition rates R_p can be generated. The output signal of the second MZM is used as the pump signal. Another CW laser centered at 1560 or 1540 nm delivers probe light that is launched into the SOA together with the pump signal. Inverted wavelength conversion is observed at the output of the band-pass filter (BPF), which is slightly detuned to the blue side of the probe wavelength (0.56 nm in this work). To realize non-inverted wavelength conversion, a silicon micro-ring resonator (MRR, with free spectral range of 200 GHz and Q value equal to 3200) is added to the output of the BPF. Typical measured eye diagrams at the output of the BPF and the MRR are shown as insets in Fig. 2. Fig. 3(a) shows the probe spectra at the outputs of the SOA and MRR, as well as the transfer functions of the BPF and the MRR. By aligning one notch of the MRR transfer function (with extinction ratio of 30 dB) to the center wavelength of the probe spectrum, the strong DC component of the probe spectrum is suppressed. In order to measure the peak power of the switched pulses and the PEs, a commercially available optical sampling oscilloscope with 1 ps time resolution is used.

2.2. SOA recovery time measurements

Fig. 3(b) shows the normalized probe traces measured at the output of the SOAs, indicating the gain recovery processes. The repetition rate of the pump pulses is 1 GHz (1 ns bit-period)

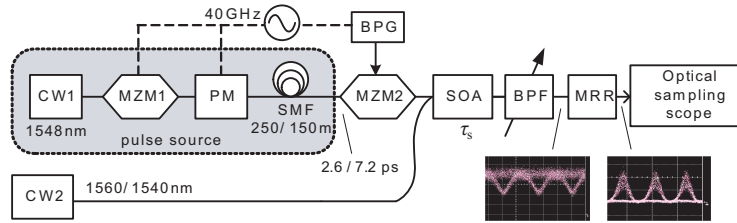


Fig. 2. Experimental setup for the PE measurements. MZM: Mach-Zehnder modulator; PM: phase modulator; SMF: standard single mode fiber; BPG: bit-pattern generator; SOA: semiconductor optical amplifier; BPF: band-pass filter; MRR: micro-ring resonator.

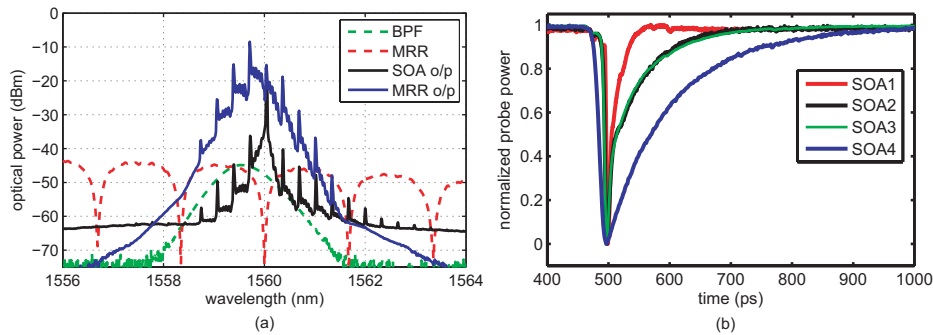


Fig. 3. (a) Optical spectra of the probe signal at the output of the SOA (black) and the MRR (blue), as well as transfer functions of the MRR (red-dashed) and the BPF (green-dashed). Pump signal: 40 Gbit/s $2^7 - 1$ PRBS. SOA2 listed in Table 1 is used. (b) Normalized probe traces at the output of the four tested SOAs for SOA recovery time measurements.

in order to make sure that the SOAs can recover fully before the injection of the next pulse. Four commercial packaged SOAs from three different companies are measured. It should be noted that the carrier density recovery process influences both the gain and the phase recovery, albeit with different recovery times. As shown later, however, a recovery parameter extracted from the slow gain recovery time does allow a good estimation of the PE saturation effects. Thus the recovery time τ_s used in this work is defined as the slow recovery component of the gain recovery process to recover from 90% to 10% of the maximum variation value. That is, the ultrafast gain compressions that can be seen in SOA1, SOA2 and SOA3 measurements due to the use of short pump pulses (2.6 ps) are excluded in the calculation of τ_s . By fitting the slow recovery part of the curves with exponential functions, the recovery times of SOA1-SOA4 are found to be 32, 121, 131 and 240 ps, respectively, as shown in Table 1 as well. Note that SOA2 and SOA3 have very similar recovery times, although they originate from different manufacturers. The operating conditions of the four SOAs, given in Table 1, are chosen so that good cross-phase modulation efficiencies are ensured for each SOA. To ensure that τ_s is exactly the recovery time that is probed in the following PE measurements, the operation conditions shown in Table 1 are also the ones used in those measurements.

2.3. Critical bit-pattern length

According to [11], a lower bound limit for the bit-pattern length that should be used to capture the maximum PE, hereafter referred to as the critical bit-pattern length n_c , is given by:

$$n_c = \lceil B \times \tau_s' \rceil + 1, \quad (1)$$

Table 1. SOA operating conditions and measured recovery times (τ_s). The probe power is 0 dBm in all cases.

| | I (mA) | pump pulse width (ps) | pump pulse energy (fJ) | probe wavelength (nm) | τ_s (ps) |
|------|-----------|--------------------------|---------------------------|--------------------------|------------------|
| SOA1 | 400 | 2.6 | 50 | 1560 | 32 |
| SOA2 | 200 | 2.6 | 25 | 1560 | 121 |
| SOA3 | 200 | 2.6 | 50 | 1560 | 131 |
| SOA4 | 500 | 7.2 | 158 | 1540 | 240 |

where B is the bit rate and $\lceil B \times \tau_s' \rceil$ denotes the minimum integer value that is larger than $B \times \tau_s'$. Note that τ_s' defined in [11] is the time needed for the carrier density variation, not the previously measured slow varying contribution to the gain, to recover from 90% to 10% of its maximum variation value. Since carrier density variations are difficult to measure, τ_s is used instead of τ_s' in Eq. (1) to calculate n_c . The following measurements show that this substitution is sufficiently accurate to estimate the magnitude of PEs. Table 2 lists the values of n_c calculated according to Eq. (1) and the estimated τ_s of Table 1. In order to justify the validity of Eq. (1), the magnitudes of the PE are measured as a function of the bit-pattern length n for SOA1-SOA4. The measured PE as a function of n are presented in two ways, i.e. for a specific SOA at different bit rates and for a specific bit rate but with different SOAs. Fig. 4(a) shows the results of the characterization of SOA2 at the bit rates of 10, 20 and 40 Gbit/s while Fig. 4(b) compares the PE of SOA1-SOA4 at 40 Gbit/s. In Fig. 4(b), the measured PEs are normalized to PE_{max} which is calculated by averaging over all the PE values for $n > n_c$. For SOA4 at 40 Gbit/s, PE at $n = 11$ is used instead of PE_{max} . PE measurements for $n > 11$ become very time consuming. In agreement with the simulation results presented in [11], the PEs increase with n but saturate gradually. The n_c estimated according to Eq. (1) are marked on Fig. 4(a) and Fig. 4(b) with star symbols. The calculated n_c show good agreement with the onset of saturation of the PE versus bit-pattern length n . Fig. 5 shows the statistics of the ratio between PE at n_c and PE_{max} for all the SOAs (identified by their recovery time τ_s). The value for SOA4 at 40 Gbit/s is not taken into account due to the difficulties in determining PE_{max} in this case. A relative difference of less than 8% is observed in all cases. Note that the absolute PE values can vary significantly from SOA to SOA and may change due to the detuning of the BPF and the MRR. However, the PE saturation characteristics are well described by the SOA recovery time and the bit rate of the input signal, confirming the effectiveness of the prediction of PE saturation using the very simple form given by Eq. (1).

Table 2. Calculated critical bit-pattern length (n_c) according to Eq. (1). The values of n_c scaled to 80 Gbit/s and 160 Gbit/s are also listed out as a reference.

| | τ_s (ps) | 10 Gbit/s | 20 Gbit/s | 40 Gbit/s | 80 Gbit/s | 160 Gbit/s |
|------|---------------|-----------|-----------|-----------|-----------|------------|
| SOA1 | 32 | 2 | 2 | 3 | 4 | 7 |
| SOA2 | 121 | 3 | 4 | 6 | 11 | 21 |
| SOA3 | 131 | 3 | 4 | 7 | 12 | 22 |
| SOA4 | 240 | 4 | 6 | 11 | 21 | 40 |

2.4. Periodic method

The basic idea of the periodic method [10, 11] is that the maximum PE can be derived by comparing the output peak power of two specific input pulse trains, corresponding to the maximum and minimum peak power of the switched pulses. To this end, the saturation conditions under

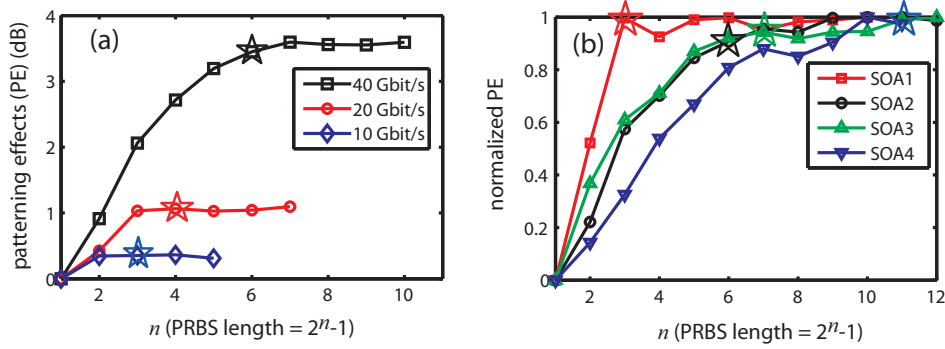


Fig. 4. (a) PE as a function of bit-pattern length (n) for SOA2. $B = 10, 20$ and 40 Gbit/s. (b) Normalized patterning effects as a function of n for $B = 40$ Gbit/s.

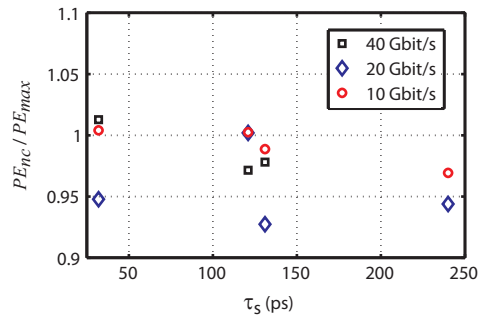


Fig. 5. Ratio of the measured PE at the critical bit-pattern length n_c , calculated according to Eq. (1), and the full PE, PE_{max} , for the four investigated SOAs (identified by their recovery time τ_s).

the two test pulse trains must be completely opposite, i.e. either unsaturated or fully saturated. According to [10], a pulse train with repetition rate R_p close to zero (or $R_p \tau_s \ll 1$) can be used for the unsaturated case while a pulse train with $R_p = B$ can be used for the fully saturated situation.

One experimental challenge was found when we attempting to verify the periodic method. Due to offset filtering, further amplification provided by an erbium-doped fiber amplifier (EDFA) is necessary after the MRR. In order to ensure that the measured peak powers of the switched pulses, hence the measured PEs, are not affected by the saturation behavior of the EDFA, a modified method is adopted in the experiment. Instead of sending two pump pulse trains at the two required repetition rates, R_p , into the SOAs separately, a synthesized pump signal is launched. It consists of 2 ns long bursts of pulses with repetition rates of 500 MHz (only one pulse is involved in this case), 10, 20 and 40 GHz, respectively, separated by 2 ns guard intervals, as shown in Fig. 6(a). The corresponding converted probe trace is shown in Fig. 6(b). Since the duration of each finite pulse train is much longer than τ_s , the peak amplitudes of the converted pulses have evolved into steady state. By recording the peak power of the steady output for each finite-duration periodic pulse train, the pattern effect estimated from the periodic method PE_{prd} can be calculated. For example, PE_{prd} at 10 Gbit/s can be calculated as the ratio of the output peak power for the 500 MHz pulse train and the peak power for the 10 GHz pulse train. Similarly, in the 20 Gbit/s case, PE_{prd} is the ratio of the peak power for the

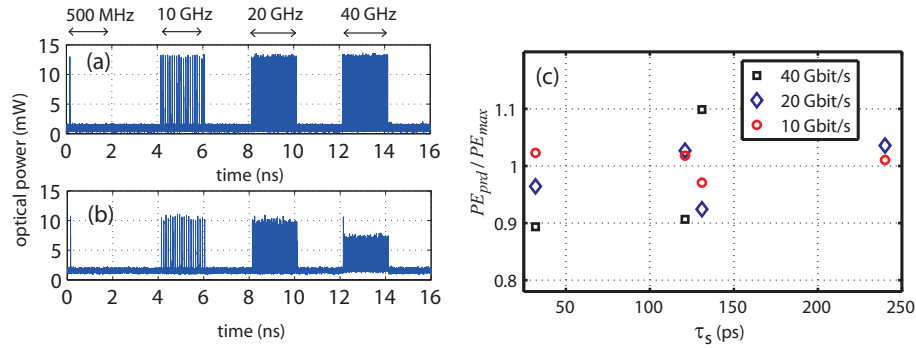


Fig. 6. (a) Test pump signal for the implementation of the periodic method and (b) corresponding converted probe signal. SOA1 is used. (c) Ratio of PE derived from the periodic method PE_{prd} and PE_{max} for the four investigated SOAs (identified by τ_s).

500 MHz pulse train and the peak power for the 20 GHz pulse train. In principle this method can be used to measure the maximum PE at an arbitrary bit rate, given that a periodic pulse train at a repetition rate equal to the bit rate can be generated. Fig. 6(c) shows the ratio between PE_{prd} and the PE_{max} measured using standard PRBS signals. The relative difference between the two results is less than 11%. Note that the experimentally adapted periodic method has the advantage of measuring the PEs at several bit rates simultaneously, making it particularly efficient. Among several possible applications, the periodic method could be used for a fast estimation of eye opening penalties induced by SOA-based switches.

3. Conclusion

In this work, we have experimentally studied the patterning effects of SOA-based ultrafast photonic switches. By measuring the dependence of the patterning effects on the bit-pattern length of the PRBSs, a characteristic saturation behavior of the PEs has been disclosed. The definition of a critical bit-pattern length indicating the saturation of the PEs has been experimentally validated for the first time and shown to result in less than 8% difference compared to PRBS measurements for a wide selection of SOAs and operation conditions. The good agreement between the theory and the measurements indicate the robustness of the proposed lower bound condition, where only the recovery times of the SOA as well as the operation bit rates are involved. A method to efficiently capture the maximum PE using only periodic bit-sequences, i.e. the periodic method, has been investigated experimentally and shows good agreement with the theory. The periodic method offers a fast and simple way to estimate the switching performance of a broad class of photonic switches.

Acknowledgement

This work was supported by VILLUM Fonden through the NATEC (Nanophotonics for Terabit Communications) Center, as well as the EU FP7 project COPERNICUS.